Dark matter in $B - L$ extended MSSM models

S. Khalil[1,2] and H. Okada[1]

[1]*Centre for Theoretical Physics, The British University in Egypt, El Sherouk City, Postal No, 11837, P.O. Box 43, Egypt*
[2]*Department of Mathematics, Ain Shams University, Faculty of Science, Cairo, 11566, Egypt*
(Received 22 November 2008; revised manuscript received 18 March 2009; published 10 April 2009)

We analyze the dark matter problem in the context of the supersymmetric $U(1)_{B-L}$ model. In this model, the lightest neutralino can be the $B - L$ gaugino $\tilde{Z}_{B-L}$ or the extra Higgsinos $\tilde{\chi}_{1,2}$ dominated. We compute the thermal relic abundance of these particles and show that, unlike the lightest neutralino in the MSSM, they can account for the observed relic abundance with no conflict with other phenomenological constraints. The prospects for their direct detection, if they are part of our galactic halo, are also discussed.

DOI: 10.1103/PhysRevD.79.083510 PACS numbers: 95.35.+d, 12.15.Lk, 12.60.Cn, 12.60.Jv

I. INTRODUCTION

Nonvanishing neutrino masses and the existence of nonbaryonic dark matter (DM) are the most important evidences of new physics beyond the standard model (SM). A simple extension of the SM, based on the gauge group $G_{B-L} \equiv SU(3)_C \times SU(2)_L \times U(1)_Y \times U(1)_{B-L}$, can account for current experimental results of light neutrino masses and their large mixing [1]. In addition, the extra-gauge boson and extra Higgs predicted in this model have a rich phenomenology and can be detected at the CERN LHC [2]. It is worth mentioning that several attempts have been proposed to extend the gauge symmetry of the SM via one or more $U(1)$ gauge symmetries beyond the hypercharge gauge symmetry [3,4].

Within supersymmetric context, it was emphasized that the three relevant physics scales related to the supersymmetry, electroweak, and baryon minus lepton $(B - L)$ breakings are linked together and occur at the TeV scale [5]. Indeed, it was shown that radiative corrections may drive the squared mass of extra $B - L$ Higgs from positive initial values at the grand unified theory (GUT) scale to negative values at the TeV scale. In such a framework, the size of the $B - L$ Higgs vacuum expectation value (VEV), responsible for the $B - L$ breaking, is determined by the size of the right-haneded Yukawa coupling and of the soft supersymmetric (SUSY) breaking terms.

In this paper, we consider the scenario where the extra $B - L$ neutralinos [three extra neutral fermions: $U(1)_{B-L}$ gaugino $\tilde{Z}_{B-L}$ and two extra Higgsinos $\tilde{\chi}_{1,2}$] can be cold DM candidates. It turns out that the experimental measurements for the anomalous magnetic moment impose a lower bound of order 30 GeV on the mass of $U(1)_{B-L}$ gaugino $\tilde{Z}_{B-L}$, while Higgsinos $\tilde{\chi}_{1,2}$ can be very light. We examine the thermal relic abundance of these particles and discuss the prospects for their direct detection if they form part of our galactic halo.

It is worth mentioning that assuming the lightest neutralino in the minimal supersymetric standard model (MSSM) as a DM candidate implies severe constraints on the parameter space of this model. Indeed, in the case of universal soft-breaking terms, the MSSM is almost ruled out by combining the collider, astrophysics, and rare decay constraints [6]. Therefore, it is important to explore very well-motivated extensions of the MSSM, such as the SUSY $B - L$ model which provides new DM candidates that may account for the relic density with no conflict with other phenomenological constraints.

The paper is organized as follows. In Sec. II we briefly review the supersymmetric $U(1)_{B-L}$ model with a particular emphasis on its extended neutralino sector. Section III is devoted for computing the lightest neutralino (LSP) annihilation cross section for $\tilde{Z}_{B-L}$, $\tilde{\chi}_1$, and $\tilde{\chi}_2$. In Sec. IV we examine the possible constraints imposed by the experimental limits of the muon anomalous magnetic moment on the mass of $\tilde{Z}_{B-L}$. We discuss the relic abundance of these DM candidates in Sec. V. We show that they can account for the measured relic density without any conflict with other phenomenological constraints. The direct detection rate of $\tilde{Z}_{B-L}$ and $\tilde{\chi}_{1,2}$ is briefly discussed in Sec. VI. Finally we give our conclusions in Sec. VII.

II. $U(1)_{B-L}$ SUSY MODEL

In the $B - L$ extension of the MSSM, the particle content includes the following fields in addition to the MSSM fields: three chiral right-handed superfields (N_i), a vector superfield associated with $U(1)_{B-L}$ (Z_{B-L}), and two chiral SM singlet Higgs superfields (χ_1, χ_2). This class of $B - L$ extension of the SM can be obtained from a unified gauge theory, like $SO(10)$, with the following branching rules for symmetry breaking: $SO(10)$ is broken down to the Pati-Salam gauge group: $SU(4)_c \times SU(2)_L \times SU(2)_R$ through the VEV of the Higgs: (1, 1, 1) in 54_H or 210_H representation at the GUT scale. Then the Pati-Salam gauge group can be directly broken down to the $B - L$ model: $SU(3)_c \times SU(2)_L \times U(1)_Y \times U(1)_{B-L}$ through the VEV of the adjoint Higgs: (15, 1, 3) below the GUT scale. Finally, the $B - L$ model is broken down to $SU(3)_c \times SU(2)_L \times U(1)_Y$ at the TeV scale as mentioned above. In this case, although the $U(1)_Y$ and $U(1)_{B-L}$ are exact symmetries at high scale (larger than TeV), they are nonor-

 © 2009 The American Physical Society

thogonal. This can be seen by noticing that the orthogonality condition [7] is not satisfied: $\sum_f Y^f Y^f_{B-L} \neq 0$, where Y^f and Y^f_{B-L} are the hypercharge and the $B-L$ charge of the fermion particle (f). In this respect, there is a kinetic mixing between the gauge fields of $U(1)_Y$ and $U(1)_{B-L}$. However, LEP results [8] stringently constrain the corresponding mixing angle to be $\lesssim 10^{-2}$. Therefore, in our analysis, we neglect this small mixing and consider the following superpotential:

$$\begin{aligned} W = {} & (Y_U)_{ij} Q_i H_u U^c_j + (Y_D)_{ij} Q_i H_d D^c_j + (Y_L)_{ij} L_i H_d E^c_j \\ & + (Y_\nu)_{ij} L_i H_u N^c_j + (Y_N)_{ij} N^c_i N^c_j \chi_1 + \mu(H_u H_d) \\ & + \mu' \chi_1 \chi_2. \end{aligned} \tag{1}$$

The $B-L$ charges of superfields that appeared in the superpotential W are given in Table I.

For universal SUSY soft-breaking terms at the grand unification scale, M_X, the soft-breaking Lagrangian, is given by

$$\begin{aligned} -\mathcal{L}_{\rm soft} = {} & m_0^2[|\tilde{Q}_i|^2 + |\tilde{U}_i|^2 + |\tilde{D}_i|^2 + |\tilde{L}_i|^2 + |\tilde{E}_i|^2 \\ & + |\tilde{N}_i|^2 + |H_u|^2 + |H_d|^2 + |\chi_1|^2 + |\chi_2|^2] \\ & + A_0[Y_U \tilde{Q}\tilde{U}^c H_u + Y_D \tilde{Q}\tilde{D}^c H_d + Y_E \tilde{L}\tilde{E}^c H_d \\ & + Y_\nu \tilde{L}\tilde{N}^c H_u + Y_N \tilde{N}^c \tilde{N}^c \chi_1] + [B(\mu H_u H_d \\ & + \mu' \chi_1 \chi_2) + \text{H.c.}] + \tfrac{1}{2} M_{1/2}[\tilde{g}^a \tilde{g}^a + \tilde{W}^a \tilde{W}^a \\ & + \tilde{B}\tilde{B} + \tilde{Z}_{B-L}\tilde{Z}_{B-L} + \text{H.c.}], \end{aligned} \tag{2}$$

where the tilde denotes the scalar components of the chiral matter superfields and fermionic components of the vector superfields. The scalar components of the Higgs superfields $H_{u,d}$ and $\chi_{1,2}$ are denoted as $H_{u,d}$ and $\chi_{1,2}$, respectively.

As shown in Ref. [5], both $B-L$ and electroweak (EW) symmetries can be broken radiatively in the supersymmetric theories. In this class of models, the EW, $B-L$, and soft SUSY breaking are related and occur at the TeV scale. The conditions for the EW symmetry breaking are given by

$$\mu^2 = \frac{m^2_{H_d} - m^2_{H_u}\tan^2\beta}{\tan^2\beta - 1} - M_Z^2/2, \qquad \sin 2\beta = \frac{-2m_3^2}{m_1^2 + m_2^2}, \tag{3}$$

where

$$\begin{aligned} & m_i^2 = m_0^2 + \mu^2, \qquad i = 1, 2 \qquad m_3^2 = -B\mu, \\ & \tan\beta = \frac{v_u}{v_d}, \qquad \langle H_u \rangle = v_u/\sqrt{2}, \qquad \langle H_d \rangle = v_d/\sqrt{2}. \end{aligned} \tag{4}$$

Here m_{H_u} and m_{H_d} are the SM-like Higgs masses at the EW scale. M_Z is a neutral gauge boson in the SM. It is worth noting that the breaking $SU(2)_L \times U(1)_Y$ occurs at the correct scale of the charged gauge boson ($M_W \sim 80$ GeV). Similarly, the conditions for the $B-L$ radiative symmetry breaking are given by [9]

$$\mu'^2 = \frac{\mu_1^2 - \mu_2^2 \tan^2\theta}{\tan^2\theta - 1} - M^2_{Z_{B-L}}/2, \qquad \sin 2\theta = \frac{-2\mu_3^2}{\mu_1^2 + \mu_2^2}, \tag{5}$$

where

$$\begin{aligned} & \mu_i^2 = m_0^2 + \mu'^2, \qquad i = 1, 2 \qquad \mu_3^2 = -B\mu', \\ & \tan\theta = \frac{v'_1}{v'_2}, \qquad \langle \chi_1 \rangle = v'_1/\sqrt{2}, \qquad \langle \chi_2 \rangle = v'_2/\sqrt{2}. \end{aligned} \tag{6}$$

Here m_{χ_1} and m_{χ_2} are the $U(1)_{B-L}$-like Higgs masses at the TeV scale. The key point for implementing the radiative $B-L$ symmetry breaking is that the scalar potential for χ_1 and χ_2 receives substantial radiative corrections. In particular, a negative squared mass would trigger the $B-L$ symmetry breaking of $U(1)_{B-L}$. It was shown that the masses of Higgs singlets χ_1 and χ_2 run differently in the way that $m^2_{\chi_1}$ can be negative whereas $m^2_{\chi_2}$ remains positive. The renormalization group equation for the $B-L$ couplings and mass parameters can be derived from the general results for SUSY renormalization group equations of Ref. [10]. After $B-L$ symmetry breaking, the $U(1)_{B-L}$ gauge boson acquires a mass [1]: $M^2_{Z_{B-L}} = 4g^2_{B-L}v'$. The high energy experimental searches for an extra neutral gauge boson impose lower bounds on this mass. The most stringent constraint on $U(1)_{B-L}$ was obtained from the LEP II result, which implies [8]

$$\frac{M_{Z_{B-L}}}{g_{B-L}} > 6 \text{ TeV}. \tag{7}$$

Now we analyze mass spectrums which have some deviations from MSSM spectrums, in particular, SM singlet Higgs bosons, the right-handed sneutrinos, and the neutralinos. The Higgs sector in the SUSY $B-L$ extension of the SM consists of two Higgs doublets and two Higgs singlets with no mixing. However, after the $B-L$ symmetry breaking, one of the 4 degrees of freedom con-

TABLE I. The $U(1)_{B-L}$ charges of the superfields.

	l	N	E	Q	U	D	H_u	H_d	χ_1	χ_2
$SU(2)_L \times U(1)_Y$	$(\mathbf{2}, -\frac{1}{2})$	$(\mathbf{1}, 0)$	$(\mathbf{1}, -1)$	$(\mathbf{2}, \frac{1}{6})$	$(\mathbf{1}, \frac{2}{3})$	$(\mathbf{1}, -\frac{1}{3})$	$(\mathbf{2}, \frac{1}{2})$	$(\mathbf{2}, -\frac{1}{2})$	$(\mathbf{1}, 0)$	$(\mathbf{1}, 0)$
$U(1)_{B-L}$	-1	-1	-1	$\frac{1}{3}$	$\frac{1}{3}$	$\frac{1}{3}$	0	0	-2	2

tained in the two complex singlets χ_1 and χ_2 are swallowed by the Z^0_{B-L} to become massive. Therefore, in addition to the usual five MSSM Higgs bosons: neutral pseudoscalar Higgs bosons A, two neutral scalars h and H, and a charged Higgs boson $H^\pm$, 3 new physical degrees of freedom remain [5]. They form a neutral pseudoscalar Higgs boson A' and two neutral scalars h' and H'. Their masses at tree level are given by

$$\begin{aligned} m^2_{A'} &= \mu_1^2 + \mu_2^2, \\ m^2_{H',h'} &= \tfrac{1}{2}(m'^2_A + M^2_{Z_{B-L}} \\ &\quad \pm \sqrt{(m^2_{A'} + M^2_{Z_{B-L}})^2 - 4m'^2_A M^2_{Z_{B-L}} \cos 2\theta}). \end{aligned} \tag{8}$$

The physical CP-even extra-Higgs bosons are obtained from the rotation of angle α:

$$\begin{pmatrix} h' \\ H' \end{pmatrix} = \begin{pmatrix} \cos\alpha & \sin\alpha \\ -\sin\alpha & \cos\alpha \end{pmatrix} \begin{pmatrix} \chi_1 \\ \chi_2 \end{pmatrix}, \tag{9}$$

where the mixing angle α is given by

$$\alpha = \frac{1}{2}\tan^{-1}\left[\tan 2\theta \frac{M'^2_A + M'^2_Z}{M'^2_A - M'^2_Z}\right]. \tag{10}$$

For $v'_1 \gg v'_2$, one finds the mixing angle α is very small, hence the above diagonalizing matrix is close to the identity. In this case, to a good approximation, one can assume that $h' \equiv \chi_1$ and $H' \equiv \chi_2$. We are going to adopt this assumption here.

Now we turn to the right-handed sneutrinos, in the basis of $(\phi_{\nu_L}, \phi_{\nu_R})$ with $\phi_{\nu_L} = (\tilde{\nu}_L, \tilde{\nu}^*_L)$ and $\phi_{\nu_R} = (\tilde{\nu}_R, \tilde{\nu}^*_R)$, the sneutrino mass matrix is given by the following 12×12 Hermitian matrix:

$$\mathcal{M}^2 = \begin{pmatrix} M^2_{\nu_L\nu_L} & M^2_{\nu_L\nu_R} \\ M^2_{\nu_R\nu_L} & M^2_{\nu_R\nu_R} \end{pmatrix}, \tag{11}$$

where $M^2_{\nu_A\nu_B}(A, B = L, R)$ can be written as

$$M^2_{\nu_A\nu_B} = \begin{pmatrix} M^2_{A^\dagger B} & M^{2*}_{A^T B} \\ M^2_{A^T B} & M^{2*}_{A^\dagger B} \end{pmatrix}, \tag{12}$$

with

$$\begin{aligned} M^2_{\nu_L^\dagger \nu_L} &= U^\dagger_{\text{MNS}} m_0^2 U_{\text{MNS}} + \frac{M_Z^2}{2}\cos 2\beta \\ &\quad + v^2 \sin^2\beta U^\dagger_{\text{MNS}}(Y^\dagger_\nu Y_\nu)U_{\text{MNS}}, \\ M^2_{\nu_R^\dagger \nu_R} &= m_0^2 + M_N^2, \\ M^2_{\nu_L^T \nu_R} &= v\sin\beta U^\dagger_{\text{MNS}} A_0(Y_N)^\dagger + v\cos\beta\mu U^\dagger_{\text{MNS}} A_0(Y_\nu)^\dagger, \\ M^2_{\nu_R^T \nu_R} &= v'\sin\theta A_0(Y_N)^\dagger, \\ M^2_{\nu_L^\dagger \nu_R} &= v\sin\beta A_0(Y_\nu)M_N, \\ M^2_{\nu_L^T \nu_L} &= 0, \end{aligned} \tag{13}$$

where $v'\sin\theta = \langle\chi_1\rangle$, $M_N = Y_N v'$, and U_{MNS} is the 3×3 unitary matrix termed the Maki-Nakagawa-Sakata (MNS) lepton mixing matrix [11]. Therefore, in general the order of magnitude of the sneutrino mass matrix is as follows:

$$\mathcal{M}^2 \sim \begin{pmatrix} \mathcal{O}(v^2) & \mathcal{O}(vv') \\ \mathcal{O}(vv') & \mathcal{O}(v'^2) \end{pmatrix}. \tag{14}$$

Since $v' \sim$ TeV, the sneutrino matrix elements are of the same order and there is no seesaw-type behavior as usually found in MSSM extended with heavy right-handed neutrinos. Therefore a significant mixing among the left- and right-handed sneutrinos is obtained. The phenomenological consequences for such mixing have been studied in [12].

Finally, we consider the neutralino sector. The neutral gaugino-Higgsino mass matrix can be written as:

$$\mathcal{M}_7(\tilde{B}, \tilde{W}^3, \tilde{H}^0_d, \tilde{H}^0_u, \tilde{\chi}_1, \tilde{\chi}_2, \tilde{Z}_{B-L}) \equiv \begin{pmatrix} \mathcal{M}_4 & \mathcal{O} \\ \mathcal{O}^T & \mathcal{M}_3 \end{pmatrix}, \tag{15}$$

where the $\mathcal{M}_4$ is the MSSM-type neutralino mass matrix and $\mathcal{M}_3$ is the 3×3 additional neutralino mass matrix, which is given by

$$\mathcal{M}_3 = \begin{pmatrix} 0 & -\mu' & -2g_{B-L}v'\sin\theta \\ -\mu' & 0 & 2g_{B-L}v'\cos\theta \\ -2g_{B-L}v'\sin\theta & 2g_{B-L}v'\cos\theta & M_{1/2} \end{pmatrix}. \tag{16}$$

As a feature of the orthogonality of $U(1)_Y$ and $U(1)_{B-L}$ in this class of models, there is no mixing between $\mathcal{M}_4$ and $\mathcal{M}_3$ at tree level. Note that in extra $U(1)$ gauged models, which are proposed to provide an explanation for the TeV scale of the μ term through the VEV of a singlet scalar, the neutralino mass matrix is given by a 6×6 matrix. If the extra singlet fermion is the lightest neutralino, then it can be an interesting candidate for dark matter, as shown in Ref. [13]. In our case, one diagonalizes the real matrix $\mathcal{M}_7$ with a symmetric mixing matrix V such as

$$V\mathcal{M}_7 V^T = \text{diag}(m_{\chi^0_k}), \qquad k = 1, \ldots, 7. \tag{17}$$

In this aspect, the LSP has the following decomposition:

$$\begin{aligned} \chi^0_1 &= V_{11}\tilde{B} + V_{12}\tilde{W}^3 + V_{13}\tilde{H}^0_d + V_{14}\tilde{H}^0_u + V_{15}\tilde{\chi}_1 \\ &\quad + V_{16}\tilde{\chi}_2 + V_{17}\tilde{Z}_{B-L}. \end{aligned} \tag{18}$$

The LSP is called pure $\tilde{Z}_{B-L}$ if $V_{17} \sim 1$ and $V_{1i} \sim 0$, $i = 1, \ldots, 6$ and pure $\tilde{\chi}_{1(2)}$ if $V_{15(6)} \sim 1$ and all the other coefficients are close to zero. In our analysis, we will focus on these two types of LSP and analyze their potential contributions to DM in the Universe. The mass eigenstates of the matrix $\mathcal{M}_3$ are in general nontrivial mixtures of the fermions $(\tilde{\chi}_1, \tilde{\chi}_2, \tilde{Z}_{B-L})$. The limit of pure $\tilde{Z}_{B-L}$ that we consider can be obtained if $v' \ll \mu'$ and the limit of pure $\tilde{\chi}_{1(2)}$ can be obtained if μ', $v' \sin(\cos)\theta \ll v' \cos(\sin)\theta$.[1]

III. LSP ANNIHILATION CROSS SECTION IN $U(1)_{B-L}$ SUSY MODEL

As advocated in the previous section, we focus on the cases where LSP is pure $\tilde{Z}_{B-L}$ or $\tilde{\chi}_{1(2)}$. In this case, the relevant Lagrangian is given by

$$-\mathcal{L}_{\tilde{Z}_{B-L}} \simeq i\sqrt{2} g_{B-L} Y^f_{B-L} \bar{\tilde{Z}}_{B-L} P_R f \tilde{f}_L + i\sqrt{2} g_{B-L} Y^f_{B-L} \bar{\tilde{Z}}_{B-L} P_L f \tilde{f}_R + \text{c.c.}, \quad (19)$$

$$-\mathcal{L}_{\tilde{\chi}_1} \simeq i\sqrt{2} g_{B-L} Y^{\chi_1}_{B-L} \bar{\tilde{\chi}}_1 \not{Z}_{B-L} \gamma_5 \tilde{\chi}_1 + i\sqrt{2} g_{B-L} Y^{\chi_1}_{B-L} \bar{\tilde{\chi}}_1 \tilde{Z}_{B-L} \chi_1 + (Y_N)_{ij} \tilde{\chi}_1 N^c{}_i \tilde{N}^c_j + \text{c.c.}, \quad (20)$$

$$-\mathcal{L}_{\tilde{\chi}_2} \simeq i\sqrt{2} g_{B-L} Y^{\chi_2}_{B-L} \bar{\tilde{\chi}}_2 \not{Z}_{B-L} \gamma_5 \tilde{\chi}_2 + i\sqrt{2} g_{B-L} Y^{\chi_2}_{B-L} \bar{\tilde{\chi}}_2 \tilde{Z}_{B-L} \chi_2 + \text{c.c.}, \quad (21)$$

where f refers to all the SM fermions, including the right-handed neutrinos. $\tilde{f}_L$ and $\tilde{f}_R$ are the left-handed and right-handed sfermions mass eignstates, respectively. Y^f_{B-L} is the $B-L$ charge defined in Table I. We assume the first right-handed neutrino N_1 is of order $\mathcal{O}(100)$ GeV; therefore the annihilation channel of the LSP into $N_1 N_1$ is also considered.

From Eq. (19), one finds that the dominant annihilation processes of $\chi^0_1 \equiv \tilde{Z}_{B-L}$ are given in Fig. 1. Our computation for the annihilation cross section leads to the following $a_{\tilde{Z}_{B-L}}$ and $b_{\tilde{Z}_{B-L}}$, where the approximation $\langle \sigma_{\text{ann}} v \rangle \simeq a + b v^2$, with v is the velocity of the incoming LSP, is assumed:

$$a_{\tilde{Z}_{B-L}} = \frac{g^4_{B-L}}{54\pi m^2_{\chi^0_1}} [\beta'_t r^2_t z^2_t + 27 \beta'_N r^2_N z^2_N], \quad (22)$$

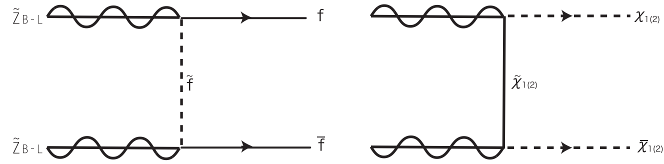

FIG. 1. The dominant annihilation cross sections in the case of the $\tilde{Z}_{B-L}$-like LSP. Note that the u channel is also taken into consideration for each diagram.

$$\begin{aligned} b_{\tilde{Z}_{B-L}} = {} & \frac{167 g^4_{B-L} \beta'_f r^2_f}{162 \pi m^2_{\chi^0_1}} (1 - 2r_f + 2r^2_f) \\ & + \frac{g^4_{B-L}}{4\pi m^2_{\chi^0_1}} \bigg[\frac{\beta'_t r^2_t}{27} \{a_1 + r_1 + z^2(a_4 + r_4)\}_t \\ & + \beta'_t r^2_t \{a_1 + r_1 + z^2(a_4 + r_4)\}_N \bigg] \\ & + \frac{4 g^4_{B-L}}{\pi m^2_{\chi^0_1}} |O_{in} O^T_{im}|^2 |V_{2,i+4} V^T_{2,i+4}|^2 \beta'_\chi r^2_\chi \\ & \times \left[\frac{4}{3} (1 + w^2_{\chi^0_2}) \beta'^2_\chi - 1 \right], \qquad (i = 1 \quad \text{or} \quad 2), \quad (23) \end{aligned}$$

$$\begin{aligned} & a_1 = \frac{2}{3} + \frac{1}{4} x^2_a z^2_a - \frac{5}{12} z^2_a, \qquad a_4 = \frac{x^2_a - 3}{4}, \\ & r_1 = \frac{r_a}{3} [-4 + z^2_a + r_a (4 - 3z^2_a - z^4_a)], \\ & r_4 = \frac{r_a}{3} (-3 + 2z^2_a + 5 r_a \beta'^2_a), \qquad z_a = m_a / m_{\chi^0}, \quad (24) \\ & w_\alpha = m_\alpha / m_{\chi^0}, \qquad r_a = (1 - z^2_a + w^2_\alpha)^{-1}, \\ & \beta'^2_a = 1 - z^2_a, \qquad x^2_a = \frac{z^2_a}{2(1 - z^2_a)}, \end{aligned}$$

where m_a is a final-state mass, m_α is a mediated-particle mass, and O is the extra Higgs mixing matrix, as defined in Eqs. (9) and (10). In our approximation, O_{in} is given by $O_{\text{in}} = \delta_{\text{in}}$, and we set $m_{\tilde{f}} \equiv m_{\tilde{f}_R} \simeq m_{\tilde{f}_L}$. Moreover, V_{2i} is the coefficient of the next LSP (NLSP). We assume that $\tilde{\chi}_{1(2)}$ is our NLSP, therefore $V_{2,i+4} \simeq 1$ ($i = 1$ or 2), $V_{2j} \simeq 0$ ($j \neq 5$ or 6). In the range of parameter space that we consider, the values of $a_{\tilde{Z}_{B-L}}$ and $b_{\tilde{Z}_{B-L}}$ are typically $\lesssim 10^{-8}$. For $m_{\tilde{Z}_{B-L}} \gtrsim 100$ GeV, the annihilation channels into extra Higgs χ_1 and χ_2 may give the dominant contributions to $b_{\tilde{Z}_{B-L}}$.

Now we turn to the Higgsino contributions. From Eq. (20), one finds that the dominant annihilation processes of $\chi^0_1 \equiv \tilde{\chi}_1$ are given in Fig. 2. The computation of the cross section leads to the following results for $a_{\tilde{\chi}_1}$ and $b_{\tilde{\chi}_1}$:

[1]We would like to thank the referee for drawing our attention to this point.

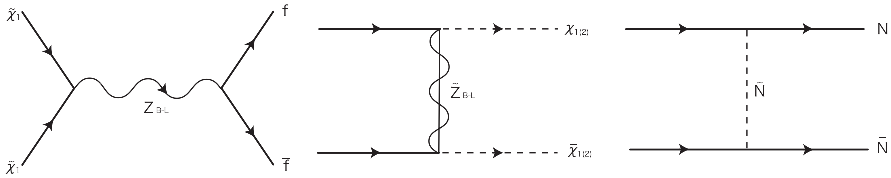

FIG. 2. The dominant annihilation channels of the $\tilde{\chi}_1$-like LSP. For the last two diagrams, the u channel is also considered.

$$a_{\tilde{\chi}_1} = \frac{\beta'_N z_N^2}{\pi}\left[\frac{(Y_{N,1m})^4 r_N^2}{32 m^2_{\chi_1^0}} + \frac{g^4_{B-L} m^2_{\chi_1^0}}{m^4_{Z_{B-L}}}\left(1-4\frac{m^2_{\chi_1^0}}{m^2_{Z_{B-L}}}\right)^{-2} + \frac{\sqrt{2}(Y_{N,1m})^2 g^2_{B-L}}{4m^2_{Z_{B-L}}}\left(1-4\frac{m^2_{\chi_1^0}}{m^2_{Z_{B-L}}}\right)^{-1}\right], \tag{25}$$

$$\begin{aligned} b_{\tilde{\chi}_1} = {}& \frac{4g^4_{B-L}}{3\pi}\frac{m^2_{\chi_1^0}}{M^4_{Z_{B-L}}}\left[\frac{23}{3}+\frac{1}{2}(1-z_t^2)\left(\frac{2}{3}+\frac{1}{4}x_t^2 z_t^2 - \frac{5}{12}z_t^2\right)\right]\left(1-4\frac{m^2_{\chi_1^0}}{M^2_{Z_{B-L}}}\right)^{-2} + \frac{\beta'_N}{\pi}\left[\frac{(Y_{N,1m})^4 r_N^2}{32m^2_{\chi_1^0}}(a_1+r_1)_N\right. \\ & \left. + \frac{g^4_{B-L} m^2_{\chi_1^0}}{m^4_{Z_{B-L}}}\left(1-4\frac{m^2_{\chi_1^0}}{m^2_{Z_{B-L}}}\right)^{-2} a_{1N}\right] + \frac{\beta'_N}{\pi}\left[\frac{\sqrt{2}(Y_{N,1m})^2 g^2_{B-L}}{4m^2_{Z_{B-L}}}\left(1-4\frac{m^2_{\chi_1^0}}{m^2_{Z_{B-L}}}\right)^{-1}\left(a_1 + r_5 z^2 - \frac{2}{3}r\beta'^2\right)_N\right] \\ & + \frac{4g^4_{B-L}}{\pi m^2_{\chi_1^0}}|O_{1n}O^T_{1m}|^2|V_{27}V^T_{27}|^2 \beta'_\chi r_\chi^2\left[\frac{4}{3}(1+w^2_{\chi_2^0})\beta'^2_\chi - 1\right]. \end{aligned} \tag{26}$$

Here V_{27} is the coefficient of NLSP. We assume that $\tilde{Z}_{B-L}$ is our NLSP, therefore $V_{27} \simeq 1$, $V_{2i} \simeq 0$ $(i \neq 7)$. We also assume $(Y_N)_{1m} \simeq (Y_N)_{11}$.

Finally we consider the annihilation process of $\chi_1^0 \equiv \tilde{\chi}_2$. From Eq. (21), one finds that $\tilde{\chi}_2\tilde{\chi}_2$ annihilation is dominated by the diagrams in Fig. 3. The computation to the cross section of $\tilde{\chi}_2$ leads to $a_{\tilde{\chi}_2} = 0$ and $b_{\tilde{\chi}_2}$ is given by

$$\begin{aligned} b_{\tilde{\chi}_2} = {}& \frac{4g^4_{B-L}}{3\pi}\frac{m^2_{\chi_1^0}}{M^4_{Z_{B-L}}}\left[\frac{23}{3}+\frac{1}{2}(1-z_t^2)\left(\frac{2}{3}+\frac{1}{4}x_t^2 z_t^2 - \frac{5}{12}z_t^2\right)\right] \\ & \times\left(1-4\frac{m^2_{\chi_1^0}}{M^2_{Z_{B-L}}}\right)^{-2} + \frac{4g^4_{B-L}}{\pi m^2_{\chi_1^0}}|O_{2n}O^T_{2m}|^2|V_{27}V^T_{27}|^2 \\ & \times \beta'_\chi r_\chi^2\left[\frac{4}{3}(1+w^2_{\chi_2^0})\beta'^2_\chi - 1\right]. \end{aligned} \tag{27}$$

It is remarkable that for $m_{\tilde{\chi}_{1,2}} \gtrsim 100$ GeV, their annihilations are dominated by the extra-Higgs channel. Therefore, $b_{\tilde{\chi}_1}$ is very close to $b_{\tilde{\chi}_2}$ and $a_{\tilde{\chi}_1}$ is quite suppressed. Thus, in this region of parameter space both $\tilde{\chi}_1$ and $\tilde{\chi}_2$ have very similar annihilation cross-section values.

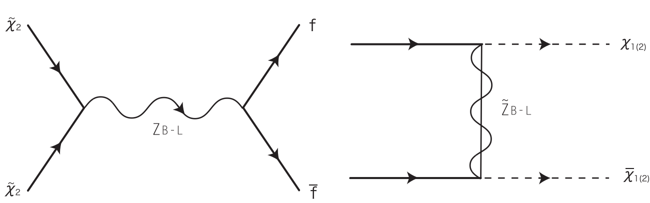

FIG. 3. The dominant annihilation cross section in the case of the $\tilde{\chi}_2$-like LSP. Note that the u channel is also taken into consideration for the t-channel diagram.

IV. CONSTRAINTS FROM MUON ANOMALOUS MAGNETIC MOMENT

In the case of $\tilde{Z}_{B-L}$-like LSP, a significant contribution to the muon anomalous magnetic moment (a_μ) may be obtained due to the 1-loop diagram mediated by $\tilde{Z}_{B-L}$ and smuon, as shown in Fig. 4. Note that $\tilde{\chi}_{1,2}$ have no direct couplings with the SM fermions, thus they do not contribute to a_μ. The recent experimental value has been determined with a very high precision by the E821 Collaboration at the National Laboratory [14]

$$a_\mu^{\rm exp} = (116\,592\,080 \pm 60) \times 10^{-11}. \tag{28}$$

This value differs from the SM prediction by the following:

$$\Delta a_\mu = a_\mu^{\rm exp} - a_\mu^{\rm SM} = (278 \pm 82) \times 10^{-11}. \tag{29}$$

Therefore, the $\tilde{Z}_{B-L}$ contribution to a_μ should satisfy the following constraints:

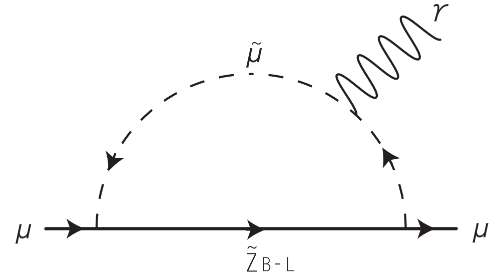

FIG. 4. $\tilde{Z}_{B-L}$ contribution to the muon anomalous magnetic dipole moment.

$$1.96 \times 10^{-9} \leq \Delta a_\mu^{\tilde{Z}_{B-L}} \leq 3.6 \times 10^{-9}. \tag{30}$$

Our computation for $\tilde{Z}_{B-L}$ contribution to a_μ leads to the following result:

$$\begin{aligned}\Delta a_\mu^{\tilde{Z}_{B-L}} = &-\frac{g_{B-L}^2}{8\pi^2}\sum_{i=1,2}\frac{m_\mu}{6m_{\tilde{\mu}_i}^2(1-s_i)^4}\Big[\sqrt{s_i}(1-s_i)(U_{\tilde{\mu}})_{2i}\\ &\times (U_{\tilde{\mu}})_{1i}Y_{B-L}^l Y_{B-L}^E 6(1-s_i^2+2s_i\ln s_i)\\ &+\frac{m_\mu}{m_{\tilde{\mu}_i}}(|(U_{\tilde{\mu}})_{2i}Y_{B-L}^E|^2+|(U_{\tilde{\mu}})_{1i}Y_{B-L}^l|^2)\\ &\times(1-6s_i+3s_i^2+2s_i^3-6s_i^2\ln s_i)\Big],\end{aligned} \tag{31}$$

where $U_{\tilde{\mu}}$ is a diagonalized unitary matrix of the slepton sector, $s_i = (m_{\chi^0}/m_{m_{\tilde{\mu}_i}})^2$ and $Y_{B-L}^{l(E)}$ is the $U(1)_{B-L}$ charge in Table I. This result is consistent with the derivation of the new contribution to a_μ in the supersymmetric $U(1)'$ model [15].

Here a few comments are in order: (i) The second term in $\Delta a_\mu^{\tilde{Z}_{B-L}}$ is suppressed by $m_\mu/m_{\tilde{\mu}_i} \simeq \mathcal{O}(10^{-3})$, while the first term is proportional to the off-diagonal elements of the diagonalized matrix $U_{\tilde{\mu}}$ which are typically of order $\mathcal{O}(10^{-2})$. Therefore the first term in Eq. (31) gives the dominant contribution to Δa_μ. (ii) From Eq. (30), the sign of the $\tilde{Z}_{B-L}$ contribution to Δa_μ should be positive. Thus $[(U_{\tilde{\mu}})_{11}(U_{\tilde{\mu}})_{21} + (U_{\tilde{\mu}})_{12}(U_{\tilde{\mu}})_{22}]Y_{B-L}^l Y_{B-L}^E$ must be negative. Note that $s_i < 1$, hence the function $f(s_i) = \sqrt{s_i}(1-s_i)(1-s_i^2+2s_i\ln s_i)$ is always positive. The elements of $U_{\tilde{\mu}}$ have a sign difference that helps in satisfying this requirement and allows for a positive contribution to Δa_μ. For example, in case $m_{\tilde{\mu}L} = m_{\tilde{\mu}R} = A \simeq 300$ GeV, $\mu = 500$ GeV and $\tan\beta = 10$, the corresponding $U_{\tilde{\mu}}$ matrix is given by

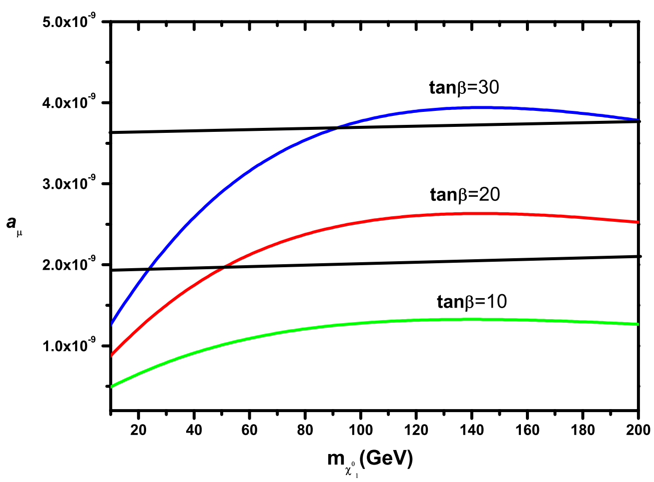

FIG. 5 (color online). $\Delta a_\mu^{\tilde{Z}_{B-L}}$ versus the mass of the LSP $\tilde{Z}_{B-L}$ for $m_{\tilde{\mu}_R} \simeq m_{\tilde{\mu}_L} \simeq A \simeq 300$ GeV, $\mu \simeq 500$ GeV with $\tan\beta = 10$, 20, and 30, and $g_{B-L} = 0.5$.

$$U_{\tilde{\mu}} \sim \begin{pmatrix} -1/\sqrt{2} & 1/\sqrt{2} \\ 1/\sqrt{2} & 1/\sqrt{2}\end{pmatrix}. \tag{32}$$

(iii) Large values of $\tan\beta$ enhance the off-diagonal elements of $U_{\tilde{\mu}}$. Hence $\Delta a_\mu^{\tilde{Z}_{B-L}}$ are enhanced by large values of $\tan\beta$.

In Fig. 5, we plot $\Delta a_\mu^{\tilde{Z}_{B-L}}$ as a function of the $\tilde{Z}_{B-L}$-like LSP mass, $m_{\chi_1^0}$, for $\tan\beta = 10$, 20, and 30. Other SUSY parameters are fixed as above. From this figure, it can be easily seen that a significant $B-L$ contribution to Δa_μ can be obtained for $\tan\beta > 10$. For $\tan\beta = 30$, the LSP mass is constrained within the region $30\ \text{GeV} < m_{\chi_1^0} < 100$ GeV. While for $\tan\beta = 20$, the allowed region of $m_{\chi_1^0}$ is wider: $m_{\chi_1^0} \gtrsim 60$ GeV.

V. LSP RELIC ABUNDANCE IN $U(1)_{B-L}$ SUSY MODEL

In this section, we compute the LSP relic abundance in the $U(1)_{B-L}$ SUSY model. We adopt the standard computation of the cosmological abundance, where the LSP is assumed to be in thermal equilibrium with the SM particles in the early universe and decoupled when it was nonrelativistic. Therefore, the LSP density can be obtained by solving the Boltzmann equation [16]:

$$\frac{dn_{\chi_1^0}}{dt} + 3Hn_{\chi_1^0} = -\langle\sigma_{\chi_1^0}^{\text{ann}}v\rangle[(n_{\chi_1^0})^2 - (n_{\chi_1^0}^{\text{eq}})^2], \tag{33}$$

where $n_{\chi_1^0}$ is the LSP number sensitivity with $m_{\chi_1^0} = \rho_{\chi_1^0}n_{\chi_1^0}$. One defines $\Omega_{\chi_1^0} = \rho_{\chi_1^0}/\rho_c$, where ρ_c is the critical mass density. It turns out that [16]

$$\begin{aligned}\Omega_{\chi_1^0}h^2 &\simeq \frac{8.76\times 10^{-11}\ \text{GeV}^{-2}}{g_{*(T_F)}^{1/2}(a/x_F + 3b/x_F^2)},\\ x_F &= \ln\frac{0.0955 m_{\text{pl}} m_{\chi_1^0}(a+6b/x_F)}{(g_{*(T_F)}x_F)^{1/2}},\end{aligned} \tag{34}$$

where m_{pl} is the Planck mass (1.22×10^{19} GeV) and $g_{*(T_F)}$ enumerates the degrees of freedom of relativistic particles at T_F. From the expressions, one notes that the LSP relic abundance depends only on the LSP mass and the annihilation cross-section coefficients a and b.

In our numerical calculation for the LSP annihilation cross section, we consider the following values of masses for the particles contributing in the process [extra-light Higgses ($\chi_{1(2)}^0$), sfermions ($\tilde{f}$), the lightest right-handed neutrino (N_1), and the NLSP (χ_2^0)]: $m_{\chi_{1(2)}} = 100$ GeV, $\tilde{f} = 200$ GeV, $N_1 = 100$ GeV, and $m_{\chi_2^0} = m_{\chi_1^0} + 30$ GeV.

In Fig. 6, we present the values of relic density Ωh^2 as a function of the LSP mass for $\tilde{Z}_{B-L}$-like LSP and $g_{B-L} \in [0.1, 0.5]$. The horizontal lines are experimentally allowed regions from the Wilkinson microwave anisotropy probe (WMAP) [17] results for cold dark matter relic density.

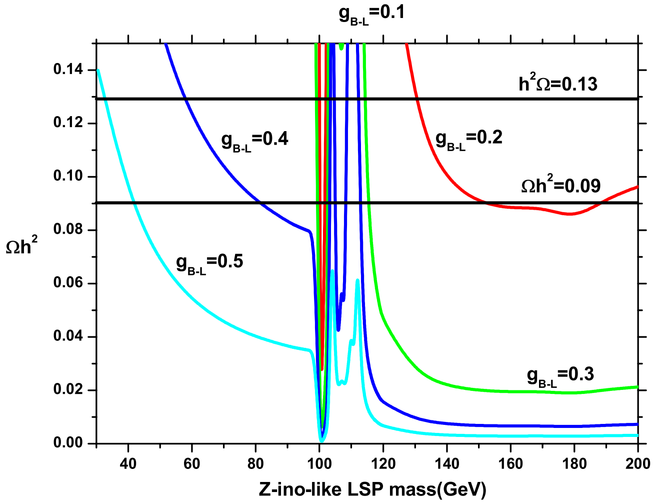

FIG. 6 (color online). Ωh^2 versus $\tilde{Z}_{B-L}$-like LSP mass for $g_{B-L} \in [0.1, 0.5]$.

Here, we have imposed the constraint on the mass of $\tilde{Z}_{B-L}$-like LSP: $m_{\tilde{Z}_{B-L}} \gtrsim 30$ GeV, due to the experimental limits on the muon anomalous magnetic moment. From this figure, one notes that since the sfermion mass is fixed at 200 GeV, the annhiliation channel due to its exchange produces a resonance at the LSP mass of order 100 GeV. For $g_{B-L} = 0.2$, the allowed region is rather wide: 130 GeV $< m_{\chi_1^0}$, while for $g_{B-L} = 0.3$, the allowed region is reduced to around 120 GeV. Finally, for $g_{B-L} \gtrsim 0.4$ a lighter LSP ($m_{\tilde{Z}_{B-L}} \lesssim 100$ GeV) is favored.

Now we turn to the Higgsino $\tilde{\chi}_{1,2}$ LSP. In Fig. 7, we plot the LSP relic density Ωh^2 as a function of $\tilde{\chi}_1$ or $\tilde{\chi}_2$ mass. As expected the relic abundance of $\tilde{\chi}_1$ or $\tilde{\chi}_2$ are quite similar since they have a very close annihilation cross section. From this figure, one notes that for $g_{B-L} \leq 0.1$, there is no essentially allowed region due to the fact that the relic abundance becomes quite large. While for $g_{B-L} = 0.2$, 0.3, 0.4, 0.5, the allowed regions for $m_{\chi_{1,2}}$ are given by [150–190], [130–135], [125–130], and [115–120] GeV, respectively.

VI. LSP DETECTION RATE IN $U(1)_{B-L}$ SUSY MODEL

In this section we analyze the effect of the event rates of our relic neutralinos ($\tilde{Z}_{B-L}$, $\tilde{\chi}_{1(2)}$) scattering off nuclei in terrestrial detectors. The direct detection experiments provide the most natural way of searching for the neutralino dark matters. The differential cross-section rate is given by [18]

$$\frac{dR}{dQ} = \frac{\sigma \rho_\chi}{2 m_{\chi_1^0} m_r^2} |F(Q)|^2 \int_{v_{\min}}^{\infty} \frac{f_1(v)}{v} dv, \qquad (35)$$

where $f_1(v)$ is the distribution of speeds relative to the detector. The reduced mass is $m_r = m_{\chi_1^0} m_N / m_{\chi_1^0} + m_N$, where m_N is the mass of the nucleus, $v_{\min} = (Q m_N / 2 m_r^2)^{1/2}$, Q is the energy deposited in the detector, and $\rho_{\chi_1^0}$ is the density of the neutralino near the Earth. It is common to fix $\rho_{\chi_1^0}$ to be $\rho_{\chi_1^0} = 0.3\ \mathrm{GeV/cm^3}$. The quantity σ is the elastic-scattering cross section of the LSP with a given nucleus. In our model, σ has two contributions: a spin-independent (scalar) contribution due to the squark exchange diagrams for $\tilde{Z}_{B-L}$-like LSP, and spin-dependent contribution arising from the Z_{B-L} gauge boson exchange diagrams for $\tilde{\chi}_{1(2)}$-like LSP. For the ^{76}Ge detector, where the total spin of ^{76}Ge is equal to zero, we have a contribution from the scalar part only, which is given by

$$\sigma^{\rm SI} = \frac{4 m_r^2}{\pi} |Z f_p + (A - Z) f_n|^2, \qquad (36)$$

where Z is the nuclear charge, and $A - Z$ is the number of

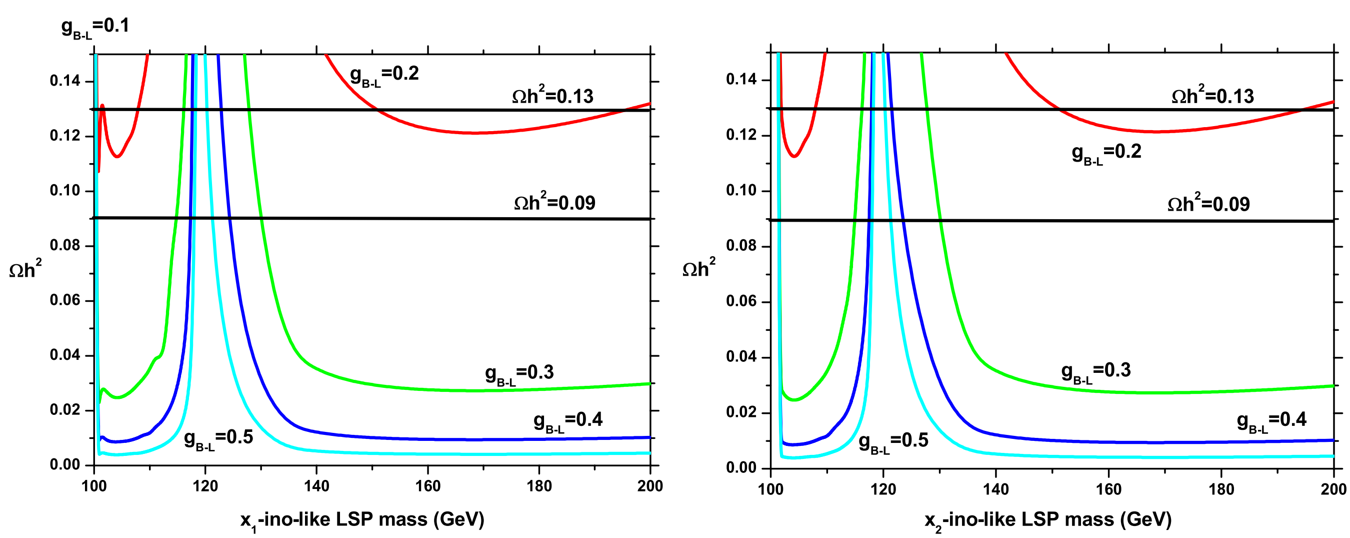

FIG. 7 (color online). Ωh^2 versus $\tilde{\chi}_{1,2}$-like LSP mass for $g_{B-L} \in [0.1, 0.5]$.

neutrons. The expressions for the effective couplings to proton and neutron, f_p and f_n, can be found in Ref. [19]. Finally, the form factor $F(Q)$, in this case is given by [18]

$$F^{\rm SI}(Q) = \frac{3j_1(qR_1)}{qR_1} e^{(-1/2)q^2 s^2}, \tag{37}$$

where $q = \sqrt{2m_N Q}$ is the momentum transferred and R_1 is given by $R_1 = (R^2 - 5s^2)^{1/2}$ with $R = 1.2\ {\rm fm} A^{1/2}$ and A is the mass number of ^{76}Ge. j_1 is the spherical Bessel function and $s \simeq 1$ fm.

For ^{76}Ge detector, where the total spin of ^{76}Ge is equal to $J = \frac{9}{2}$, we have a contribution from the spin-dependent part only, which can be written as

$$\sigma^{\rm SD}|F^{\rm SD}(Q)|^2 = \frac{4m_r^2}{2J+1}[(f_p^a)^2 S_{pp}(q) + (f_n^a)^2 S_{nn}(q) + f_p^a f_n^a S_{pn}(q)], \tag{38}$$

where $S_{pp}(q) = S_{00}(q) + S_{11}(q) + S_{01}(q)$, $S_{nn}(q) = S_{00}(q) + S_{11}(q) - S_{01}(q)$, and $S_{pn}(q) = 2[S_{00}(q) - S_{11}]$, and the expressions for f_p^a and f_n^a can be found in Ref. [20]. The values of the spin structure functions $S_{00}(q)$, $S_{11}(q)$, and $S_{01}(q)$ are given in [19].

In the case of the $\tilde{Z}_{B-L}$-like LSP, the effective couplings to the proton and neutron are very similar, i.e., $f_p \simeq f_n$. Therefore, the cross section, $\sigma^{\rm SI} \equiv \sigma^{\rm SI}_{\tilde{Z}_{B-L}}$, is given by

$$\sigma^{\rm SI}_{\tilde{Z}_{B-L}} \simeq \frac{4m_r^2}{\pi}\left|\sum_q \frac{1}{2}\langle N|\bar{q}q|N\rangle \sum_{k=1}^{6} \frac{g_{\tilde{q}_{L_k}\chi q}\, g_{\tilde{q}_{R_k}\chi q}}{m^2_{\tilde{q}_k}}\right|^2, \tag{39}$$

where q refers to u, d, s, c, b, and t. The hadronic matrix elements are given by $\langle N|\bar{q}q|N\rangle = f^p_{T_q} m_p/m_q$. The values of the parameters $f^p_{T_q}$ can be found in Ref. [20]. From Eq. (19), one finds that $\tilde{Z}_{B-L}$ couples universally to all type of quarks, i.e., $g_{\tilde{q}_{L_k}\chi q} = g_{\tilde{q}_{R_k}\chi q} \simeq i\sqrt{2} g_{B-L} Y^q_{B-L}$.

In Fig. 8, we present our numerical results for the event rate R as a function of $\tilde{Z}_{B-L}$-like LSP mass for $m_{\tilde{q}} = 200$ GeV and $g_{B-L} \in [0.1, 0.5]$. As can been seen from this figure, the detection rates are quite sensitive to the value of gauge coupling g_{B-L}. This is due to the fact that R depends on the fourth power of g_{B-L}. Nevertheless, the detection rates are less than 10^{-3} events/kg/day, which are below the current experimental limit: 0.01 events/kg/day [21]. Thus, one can conclude that $\tilde{Z}_{B-L}$ is beyond the reach of near future experiments.

Now we turn to the case of $\tilde{\chi}_{1(2)}$-like LSP. As mentioned above, in this case the scattering cross section is given by the spin-dependent part: $\sigma^{\rm SD} \equiv \sigma^{\rm SD}_{\tilde{\chi}_{1(2)}}$, which is given by Eq. (38) with

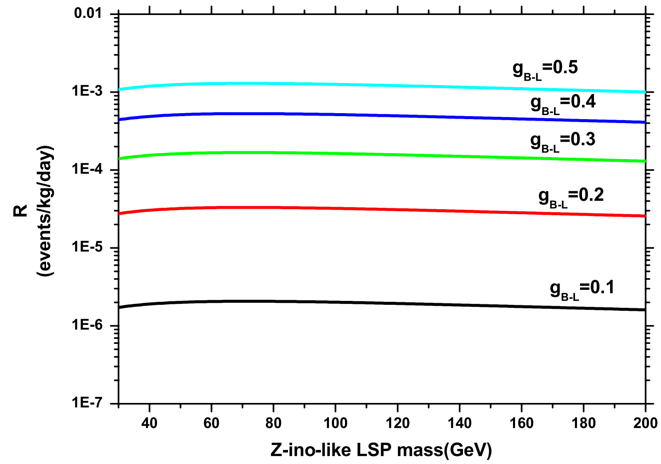

FIG. 8 (color online). Detection rate versus $\tilde{Z}_{B-L}$-like LSP mass for $g_{B-L} \in [0.1, 0.5]$. As in the previous figures, $m_{\tilde{q}} = 200$ GeV is assumed.

$$f_N^a = \sum_{q=u,d,s} (\Delta q)_N \left(\frac{2g^2_{B-L} Y^\chi_{B-L} Y^q_{B-L}}{m^2_{Z_{B-L}}}\right) \lesssim \frac{2}{3}\left(\frac{1}{6000\ {\rm GeV}}\right)^2 \sum_{q=u,d,s} (\Delta q)_N. \tag{40}$$

Here we have used the lower limit on the ratio: $M_{Z_{B-L}}/g_{B-L}$ reported in Eq. (7). The numerical values of $S_{00}(q)$, $S_{11}(q)$, $S_{01}(q)$, and $(\Delta q)_N$ can be found in Ref. [20]. From this expression, it is clear that the detection rates of the extra Higgsinos-like LSP are extremely small. They are typically less than 10^{-16} (events/kg/day). This result is consistent with the spin-dependent contribution for the singlino in SUSY models with $U(1)'$ [22,23]. However, in this class of model, unlike our $U(1)_{B-L}$ model, the singlino dominated LSP may imply large detection rates, due to the spin-independent contributions.

VII. CONCLUSIONS

We have studied the DM problem in supersymmetric $B-L$ extension of the SM. We showed that the extra $B-L$ neutralinos [three extra neutral fermions: $U(1)_{B-L}$ gaugino $\tilde{Z}_{B-L}$ and two Higgsinos $\tilde{\chi}_{1,2}$] are interesting candidates for cold DM. We provided analytic expressions for their annihilation cross sections. We also computed the $\tilde{Z}_{B-L}$ contribution to the muon anomolous magnetic moment and showed that the current experimental limits impose a lower bound of order 30 GeV on $\tilde{Z}_{B-L}$ mass. We analyzed the thermal relic abundance of both $\tilde{Z}_{B-L}$ and $\tilde{\chi}_{1,2}$. We showed that unlike the LSP in MSSM, these particles can account for the measured relic abundance with no conflict with other phenomenological constraints. Finally, we discussed their direct detection rates and showed that they are beyond the reach of our near future experiments.

ACKNOWLEDGMENTS

We thank D. A. Demir for discussions. H. O. would like to thank Y. Daikoku, S. Nakamura, and Y. Kajiyama for interesting comments. This work was partially supported by the ICTP Grant No. Proj-30 and the Egyptian Academy for Scientific Research and Technology.

---

[1] S. Khalil, J. Phys. G **35**, 055001 (2008).
[2] M. Abbas and S. Khalil, J. High Energy Phys. 04 (2008) 056; W. Emam and S. Khalil, Eur. Phys. J. C **52**, 625 (2007); K. Huitu, S. Khalil, H. Okada, and S. K. Rai, Phys. Rev. Lett. **101**, 181802 (2008); S. Khalil and O. Seto, J. Cosmol. Astropart. Phys. 10 (2008) 024.
[3] Vernon D. Barger, Ernest Ma, and K. Whisnant, Phys. Rev. D **26**, 2378 (1982).
[4] R. N. Mohapatra and R. E. Marshak, Phys. Rev. Lett. **44**, 1316 (1980); R. E. Marshak and R. N. Mohapatra, Phys. Lett. **91B**, 222 (1980); C. Wetterich, Nucl. Phys. **B187**, 343 (1981); A. Masiero, J. F. Nieves, and T. Yanagida, Phys. Lett. **116B**, 11 (1982); R. N. Mohapatra and G. Senjanovic, Phys. Rev. D **27**, 254 (1983); R. E. Marshak and R. N. Mohapatra, *From Su(3) to Gravity*, edited by E. Gotsman and G. Tauber (Univ. Pr., Cambridge, UK, 1985), pp. 173–181; W. Buchmuller, C. Greub, and P. Minkowski, Phys. Lett. B **267**, 395 (1991).
[5] S. Khalil and A. Masiero, Phys. Lett. B **665**, 374 (2008).
[6] J. R. Ellis, K. A. Olive, Y. Santoso, and V. C. Spanos, Phys. Lett. B **565**, 176 (2003).
[7] Will Loinaz and Tatsu Takeuchi, Phys. Rev. D **60**, 115008 (1999).
[8] M. Carena, A. Daleo, B. A. Dobrescu, and T. M. P. Tait, Phys. Rev. D **70**, 093009 (2004).
[9] S. Khalil and Q. Shafi, Nucl. Phys. **B564**, 19 (2000).
[10] S. P. Martin and M. T. Vaughn, Phys. Rev. D **50**, 2282 (1994); **78**, 039903 (2008); see also K. Inoue, A. Kakuto, H. Komatsu, and S. Takeshita, Prog. Theor. Phys. **68**, 927 (1982); **70**, 330(E) (1983); J. R. Ellis, J. S. Hagelin, D. V. Nanopoulos, and K. Tamvakis, Phys. Lett. **125B**, 275 (1983); L. E. Ibanez and C. Lopez, Phys. Lett. **126B**, 54 (1983); L. Alvarez-Gaume, J. Polchinski, and M. B. Wise, Nucl. Phys. **B221**, 495 (1983); T. Kikuchi and T. Kubo, Phys. Lett. B **666**, 262 (2008).
[11] Z. Maki, M. Nakagawa, and S. Sakata, Prog. Theor. Phys. **28**, 870 (1962).
[12] Y. Grossman and H. E. Haber, Phys. Rev. Lett. **78**, 3438 (1997).
[13] D. Jarecka, J. Kalinowski, S. F. King, and J. P. Roberts, arXiv:0709.1862, ECONF C0705302, SUS15 (2007); J. Kalinowski, S. F. King, and J. P. Roberts, J. High Energy Phys. 01 (2009) 066.
[14] G. W. Bennett *et al.* (Muon g-2 Collaboration), Phys. Rev. D **73**, 072003 (2006); arXiv:hep-ph/9707451.
[15] Y. Daikoku, arXiv:hep-ph/0107305.
[16] K. Griest, Phys. Rev. D **38**, 2357 (1988).
[17] C. L. Bennett *et al.* (WMAP Collaboration), Astrophys. J. Suppl. Ser. **148**, 1 (2003); D. N. Spergei *et al.* (WMAP Collaboration), Astrophys. J. Suppl. Ser. **148**, 175 (2003).
[18] S. Khalil, A. Masiero, and Q. Shafi, Phys. Rev. D **56**, 5754 (1997).
[19] Gerard Jungman, Marc Kamionkowski, and Kim Griest, Phys. Rep. **267**, 195 (1996).
[20] P. Gondolo, J. Edsjo, P. Ullio, L. Bergstrom, Mia Schelke, and E. A. Baltz, J. Cosmol. Astropart. Phys. 07 (2004) 008.
[21] Z. Ahmed *et al.* (CDMS Collaboration), Phys. Rev. Lett. **102**, 011301 (2009).
[22] V. Barger, P. Langacker, lan Lewis, Mat McCaskey, G. Shaughnessy, and B. Yencho, Phys. Rev. D **75**, 115002 (2007).
[23] B. de Carlos and J. R. Espinosa, Phys. Lett. B **407**, 12 (1997).